RSC Advances

PAPER

View Article Online
View Journal | View Issue

Cite this: *RSC Adv.*, 2025, **15**, 9587

Reversible color changing response of pyrenylated charge-transfer probes towards Hg^{2+}: linker-driven modulation of sensitivity and selectivity†

Nilanjan Dey *

Two easily synthesizable prenylated charge transfer probes with a terminal pyridine unit were designed. The compounds differ based on the nature of the spacer: rigid olefinic (**1**) and flexible hydrazo (**2**). Both compounds show exclusive interaction with Hg^{2+} ions, leading to changes in visible color. Experimental analyses showed that compound **1** outperformed compound **2** in terms of sensitivity ($A/A_0 \sim$ 13-fold *vs.* ~2-fold) and detection limit (1.2 ppm *vs.* 5.8 ppm), attributed to its rigid linker and enhanced binding affinity. Moreover, ratiometric responses ($r^2 > 0.99$) and excellent selectivity for Hg^{2+} were demonstrated. This study highlights the development of robust, reusable, and cost-effective tools for mercury detection, thus addressing critical environmental and health concerns associated with mercury contamination. Environmental robustness of compound **1** was validated across solvents, counter-ions, and water mixtures, with decreasing efficacy in high-water-content systems owing to solvation effects and probe aggregation. Mechanistic studies confirmed pyridine nitrogen as the primary coordination site with reversible binding, enabling probe reuse. Practical applications were explored using paper strips modified with the probes, which facilitated rapid, cost-effective, and quantitative detection of Hg^{2+} *via* image analysis.

Received 22nd November 2024
Accepted 15th January 2025

DOI: 10.1039/d4ra08302d

rsc.li/rsc-advances

Introduction

Charge transfer (CT)-based probes are invaluable for the optical sensing of heavy metal pollutants because of their high sensitivity, selectivity, and rapid response, enabling detection at concentrations as low as nanomolar levels, often below regulatory limits for pollutants such as Hg^{2+} (2 ppb set by the EPA) or Pb^{2+} (15 ppb set by the EPA).[1] Tailored with specific functional groups, these probes offer exceptional selectivity for metals such as Hg^{2+}, Pb^{2+}, or Ag^{+} and produce rapid, often visible optical changes with detection times typically under minutes, facilitating on-site detection without complex equipment. Their versatility allows them to function across diverse conditions, such as pH ranges of 4–10 or in high ionic strength environments, providing mechanistic insights into metal–probe interactions and advancing sensor design.[2] Moreover, CT-based probes can be integrated into portable formats such as paper strips or hydrogels, achieving detection limits as low as 10^{-9} M.[3] Recent innovations incorporate smartphone-enabled imaging and machine learning for enhanced data interpretation.[4]

The spacer group in charge transfer (CT)-based probes plays a pivotal role in modulating their electronic and optical properties, directly influencing their colorimetric sensing capabilities. The nature of the spacer dictates how efficiently the donor and acceptor groups interact. Conjugated linkers often enhance electronic communication, leading to red-shifted absorption spectra and a more sensitive response to analytes. However, non-conjugated linkers reduce electronic coupling, weakening CT efficiency but often increasing selectivity towards target analytes by minimizing background interference.[5] Similarly, flexibility of the spacer can affect sensing performance. Flexible spacers allow the probe to adopt various conformations, potentially improving analyte binding. However, this flexibility may result in less stable and reproducible responses. Rigid spacers, on the contrary, maintain a fixed spatial arrangement of donor and acceptor groups, ensuring consistent CT behavior and reliable colorimetric response.[6] Moreover, the length of the spacer influences the strength of electronic interactions. Short spacers enhance CT efficiency by facilitating strong electronic overlap between donor and acceptor groups, resulting in intense optical changes upon analyte binding. In contrast, long spacers reduce electronic overlap, weakening CT and shifting absorption or emission to shorter wavelengths.[7] Moreover, longer spacers can improve selectivity by spatially separating reactive sites, reducing nonspecific interactions.

Despite such important roles of spacers in the optical properties of CT probes and sensing efficacy, not many systematic investigations have been carried out focusing on this aspect. Therefore, herein, we designed pyrene-based, easily

Department of Chemistry, Birla Institute of Technology and Science Pilani, Hyderabad, Telangana-500078, India. E-mail: nilanjan@hyderabad.bits-pilani.ac.in

† Electronic supplementary information (ESI) available. See DOI: https://doi.org/10.1039/d4ra08302d

synthesizable charge-transfer probes with pyridine as the metal ion binding site (Fig. 1a). Two compounds with different spacers (olefinic *vs.* hydrazo) were considered with the same donor (pyrene) and acceptor (pyridine) moieties. Such variations in the spacer unit showed distinct influence on the optical properties of the compounds and efficacy towards Hg^{2+} sensing. Binding with Hg^{2+} ions would facilitate charge transfer from the donor to acceptor moiety, leading to changes in visible color (Fig. 1b). In addition to solution-based analysis, the paper attempted rapid, on-location detection of Hg^{2+} using chemically modified paper strips. The quantitative analysis in this case was achieved using ImageJ (free version).

Results and discussion

Design and synthesis

In this work, we designed two easily synthesizable prenylated probes with pyridine as the terminal functional group.[8] The two compounds differed based on the nature of the linker unit connecting the donor and acceptor sites. In case of compound **1**, the electron-rich pyrene unit is linked with electron-deficient pyridine residue *via* a *trans* olefinic bond, while the same units are connected *via* a hydrazo spacer in compound **2**. Both compounds showed a color in the visible region, attributed to intramolecular charge transfer from pyrene to pyridine unit. Therefore, any change in the electronic nature of the pyridine unit would be expected to influence the optical response of the probe molecules. The olefinic linker, with its conjugated and planar structure, is expected to promote efficient π-electron delocalization between the donor and acceptor units, resulting in enhanced charge transfer (CT) and higher sensitivity to changes in the electronic environment caused by metal ion binding. However, the hydrazo linker, containing lone pair-bearing nitrogen atoms, disrupts π-conjugation but provides an additional coordination site for metal ions. The rigid structure of the olefinic linker supports higher fluorescence quantum yields, while the flexible hydrazo linker allows for conformational adaptability, enhancing metal ion chelation.

The energy optimization of compounds **1** and **2** was carried out using B3LYP level of theory with the 6-31G* basis set.[9] Both compounds demonstrated a nearly planar structure with dihedral angles of <0.2° between the spacer and donor (or acceptor) moieties (Fig. 2a). The HOMO–LUMO energy gap was calculated for **1** and **2** and was found to be in the similar range ($\Delta E \sim 0.12$ eV) (Fig. 2b). Further, we calculated Mulliken charge distribution in the pyridine ring. For both compounds, the pyridyl nitrogen ends appeared to have high negative charge density, suitable for metal ion coordination (Fig. 2c and d).

Spectroscopic response in the solution phase

The UV-visible spectra of compounds **1** and **2** were recorded in acetonitrile. The UV-visible spectrum of compound **1** showed two distinct absorption bands at 287 ($\varepsilon = 2.58 \times 10^5\ M^{-1}\ cm^{-1}$) and 373 ($\varepsilon = 4.05 \times 10^5\ M^{-1}\ cm^{-1}$) nm owing to π–π* transition and charge transfer interaction, respectively. For compound **2**, both these bands appeared to be slightly red-shifted and were observed at 291 ($\varepsilon = 2.90 \times 10^5\ M^{-1}\ cm^{-1}$) and 380 ($\varepsilon = 3.39 \times 10^5\ M^{-1}\ cm^{-1}$) nm, respectively. Moreover, an additional absorption band was found at a lower energy region, centered at 408 nm ($\varepsilon = 2.64 \times 10^5\ M^{-1}\ cm^{-1}$) (Fig. 3a). The lone pairs on the nitrogen atoms of the hydrazo unit could facilitate charge-transfer interaction, leading to the formation of a red-shifted absorption band.[10] Moreover, the hydrazo compound can form hydrogen bonding with polar protic solvents and form self-assembled aggregated structures. However, the fluorescence spectrum of **1** showed broad emission band in the 457 nm region. Although emission maximum was observed at a similar position for compound **2**, the intensity was found to be significantly less (~4.6-fold) (Fig. 3b). The higher flexibility of the hydrazo linker probably enhances the possibilities of non-radiative decay, which resulted in low fluorescence intensity.[11] Furthermore, to compare the metal ion binding efficiency of **1** and **2**, we recorded ^{1}H-NMR spectra of both compounds in DMSO-d_6 (Fig. 3c). We could not record the spectrum in CD_3CN owing to limited solubility at room temperature. The aromatic protons of compound **2** adjacent to pyridine nitrogen ends (a and b) appeared in the deshielded region compared to compound **1**. This suggested that the pyridine ring in the case of compound **2** is relatively electron deficient. Moreover, the imine protons in **2** expectedly showed a considerable downfield shift compared to olefinic protons of **1**. Consequently, there is a possibility that probe **2** would not bind with metal ions as effectively as compound **1**.

Chromogenic response towards Hg^{2+} ions

We investigated the metal ion binding properties of compounds in acetonitrile. When compound **1** was exposed to Hg^{2+} ions, the color of the solution immediately changed to yellow. Expectedly,

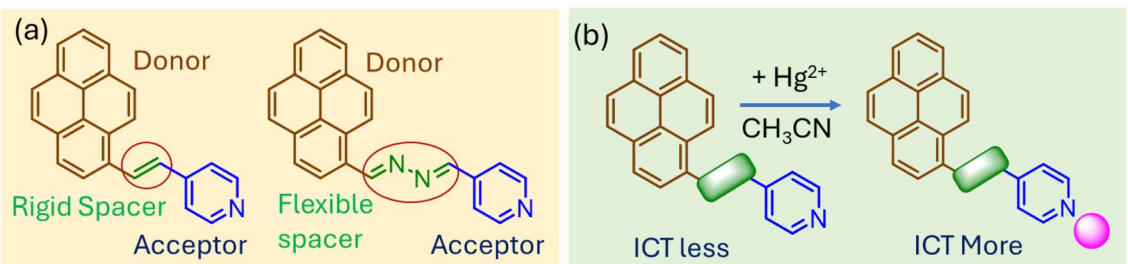

Fig. 1 (a) Chemical structures of probe molecules involved in the present study. (b) Shows plausible binding interaction with Hg^{2+} ions.

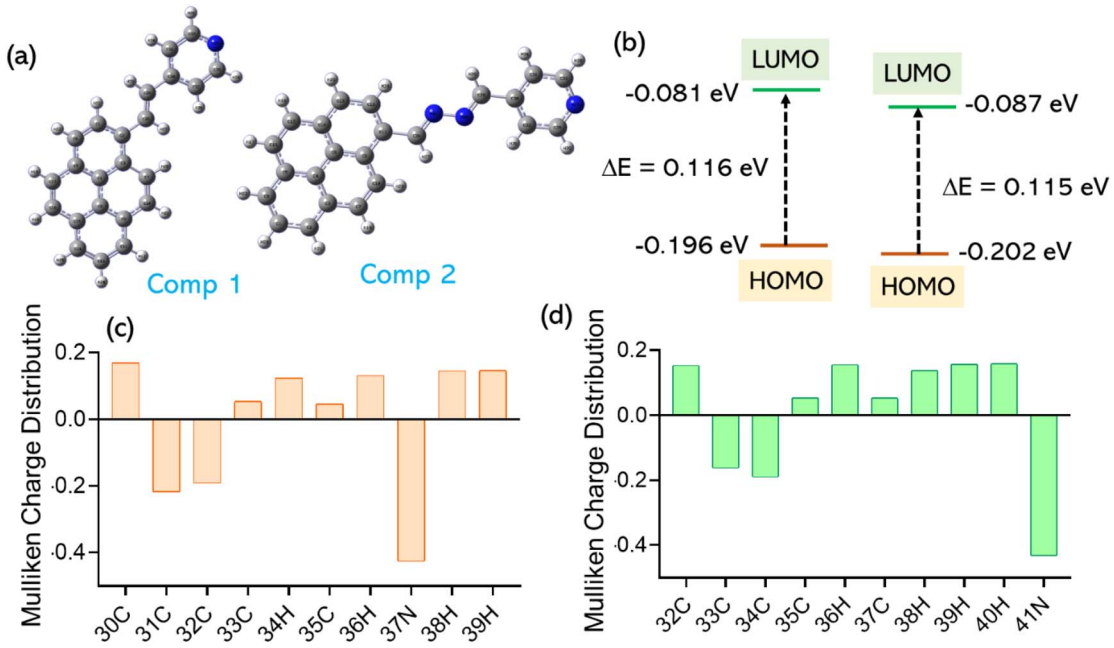

Fig. 2 (a) Energy-optimized structures of **1** and **2** using B3LYP/6-31G* level of theory. (b) Schematic showing relative HOMO–LUMO energy levels for compounds **1** and **2**. Mulliken charge distribution on the pyridine ring for compounds (c) **1** and (d) **2**.

the UV-visible spectrum with Hg^{2+} showed formation of a new band at the 427 nm region. Titration studies showed that the absorbance at 427 nm enhanced with an increasing concentration of Hg^{2+} ions at the expense of the 375 nm band (Fig. 4a). The isosbestic points were found at 328 and 392 nm, indicating a one-to-one equilibrium between **1** and Hg^{2+} ions.

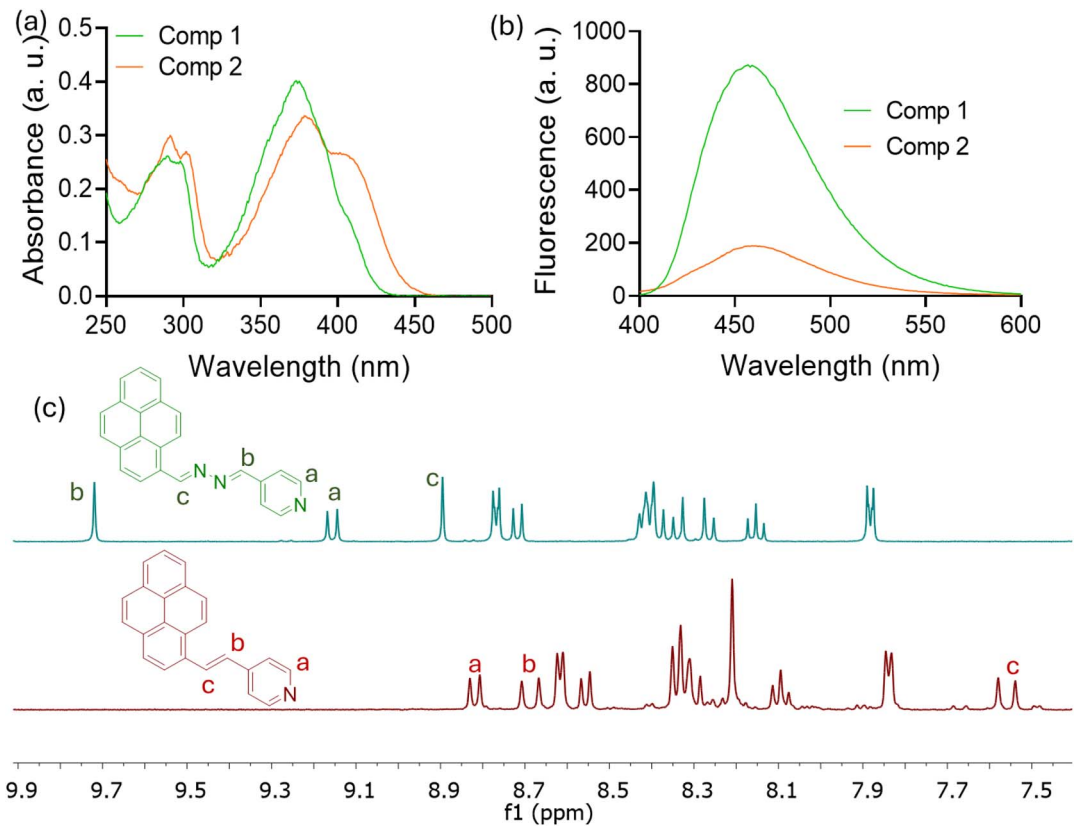

Fig. 3 (a) UV-visible spectra of **1** and **2** (10 μM) in CH_3CN. (b) Fluorescence spectra of **1** and **2** (10 μM, $\lambda_{ex} = 375$ nm) in CH_3CN. (c) Partial ^{1}H-NMR spectra of **1** and **2** (5 mM) in DMSO-d_6 (inset shows structures of compounds **1** and **2** with assigned protons).

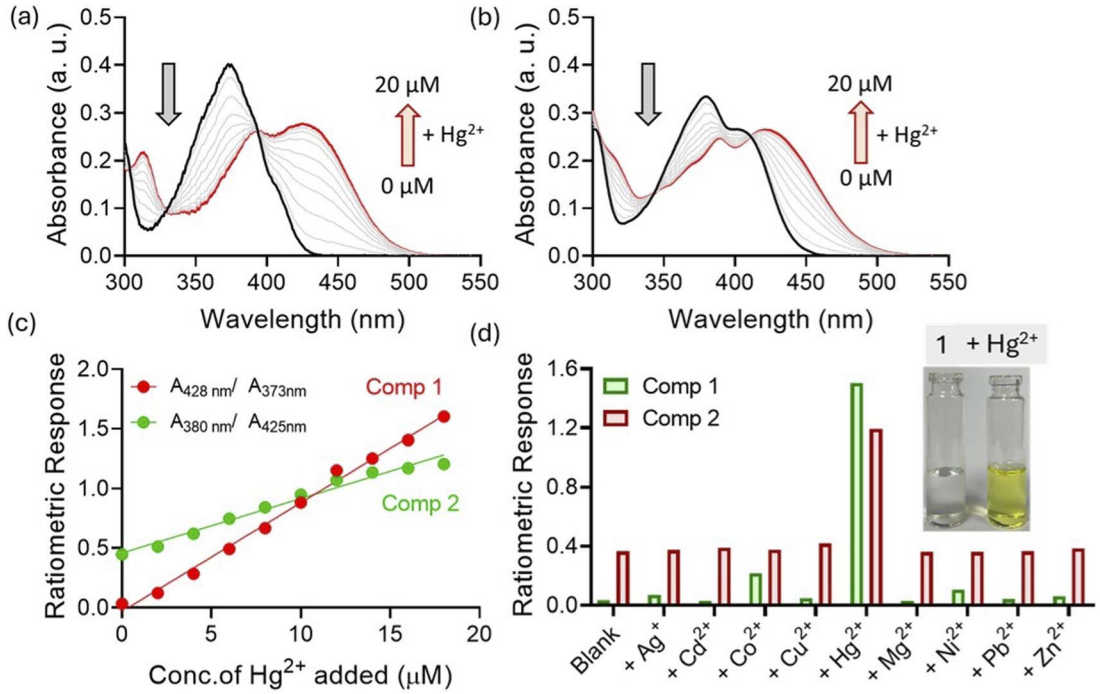

Fig. 4 UV-visible titration of (a) **1** and (b) **2** (10 μM) with Hg^{2+} (0–20 μM) in a CH_3CN medium. (c) Ratiometric responses of **1** and **2** (10 μM) towards Hg^{2+} ions (0–20 μM) in a CH_3CN medium. (d) Ratiometric responses of **1** and **2** (10 μM) in the presence of various metal ions (25 μM) in a CH_3CN medium [each experiment was independently performed thrice for reproducibility].

When compound **2** was subjected to Hg^{2+} ions, we witnessed a new charge transfer band at 423 nm. Here, titration studies showed that absorbance at the 423 nm band enhanced concomitantly with quenching at 378 and 404 nm bands (Fig. 4b). In this case, isosbestic points were observed at 343 and 410 nm. Interestingly, comparison studies indicated that the charge transfer band for compound **1** was found to be more prominent ($A/A_0 \sim 13$ fold at 427 nm) than that witnessed with compound **2** ($A/A_0 \sim 2$ fold at 423 nm). Furthermore, we plotted the ratiometric responses of compounds **1** ($Abs_{428\ nm}/Abs_{373\ nm}$) and **2** ($Abs_{423\ nm}/Abs_{380\ nm}$) against the concentrations of Hg^{2+} added (Fig. 4c). In both cases, we observed linear regression ($r^2 > 0.99$), which indicated the ratiometric nature of the probe molecules. This is particularly important for real-life sample analysis as ratiometric probes by considering responses at different wavelengths can minimize background interferences and improve the signal-to-noise ratio.[12] Moreover, we noted that changes in the response were prominent with compound **1** compared with compound **2**. Since selectivity is one of the most important criteria for quantitative analysis, we analysed interactions of compounds **1** and **2** with other metal ions under similar conditions. For both compounds, no other metal ions could show changes in the absorption signal as prominently as that observed with Hg^{2+} ions (Fig. 4d). This indicated that both sensors **1** and **2**, irrespective to the differences in the sensitivity, showed good selectivity towards Hg^{2+} ions in the solution phase. Furthermore, UV-visible titration studies indicated that the limits of detection for Hg^{2+} ions were 0.012 and 0.02 ppm with probes **1** and **2**, respectively.

Time-dependent studies indicate that the perceptible color change of **1** with Hg^{2+} ions could be seen within 30 s of Hg^{2+} ion addition. However, the color response was found to be quite stable and no further change in absorbance was noted even after 1 h of Hg^{2+} addition (Fig. S1†). This indicated that the present method is robust and can produce reliable spectroscopic signals for Hg^{2+} ions. Considering that traditional solution-based sensing studies need sophisticated instrumental facilities and trained technicians, we developed an alternative strategy for Hg^{2+} detection using chemically modified precoated paper strips.[13] The paper strips in the native state showed no color under day-light. However, when the paper strip was exposed to Hg^{2+} ions, the color of the strip changed to yellow (Fig. 5a). This observation indicated that detection of Hg^{2+} was indeed possible on a solid surface. Furthermore, the changes in the color of the paper strips were quantitatively assessed by ImageJ.[14] It was observed that the paper strips spiked with Hg^{2+}-contaminated solution can be reused upon washing with diluted EDTA solution. Since this method does not involve multi-step sample preparation, involvement of skilled technicians or analysis of complex signal output, people with limited knowledge of science or technology will be able to use it without much difficulty.

Effect of the microenvironment on Hg^{2+}-ion sensing

Considering the selective interaction, we further investigated effects of different environmental and other factors on the efficacy of Hg^{2+} detection by compound **1**. First, we checked the interaction of compound **1** with different Hg^{2+} salts (with $-NO_3$

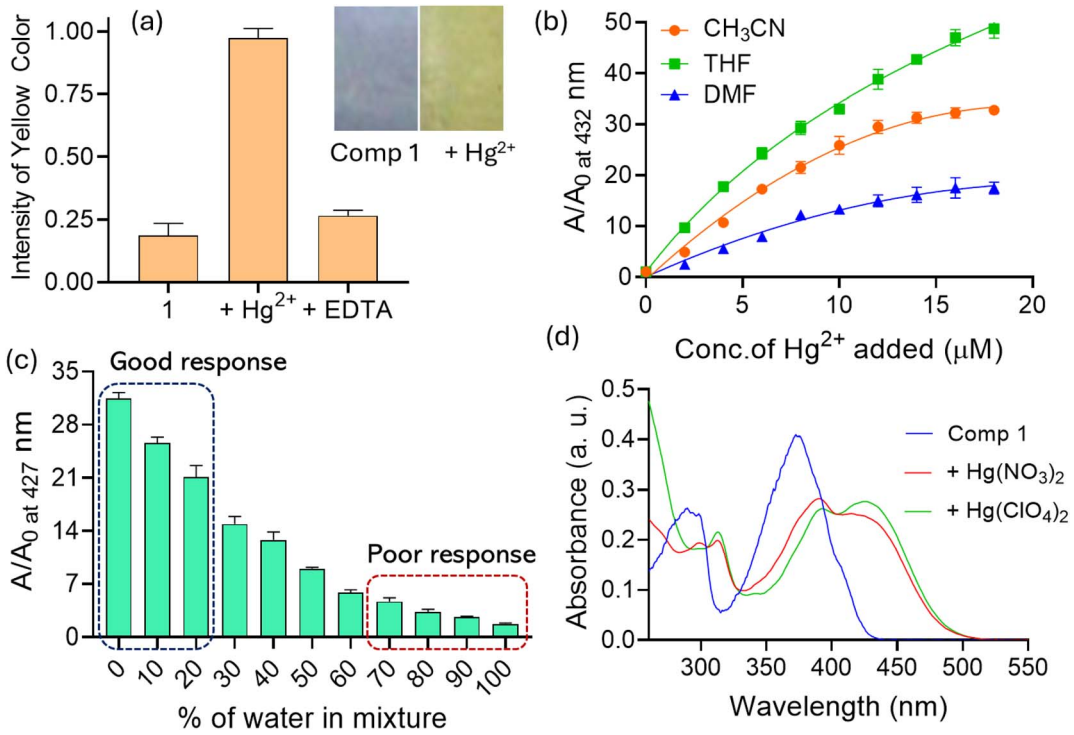

Fig. 5 (a) Reusable paper strips (coated with compound **1**) for detection of Hg^{2+} ions. (b) Changes in absorbance of **1** (10 μM) upon addition of Hg^{2+} (0–20 μM) in different organic media. (c) Changes in absorbance at the 427 nm band with Hg^{2+} ions in different CH_3CN–H_2O mixtures. (d) UV-visible spectra of **1** (10 μM) with different Hg^{2+} salts (25 μM) in a CH_3CN medium [each experiment was independently performed thrive for reproducibility].

and $-ClO_4$ counter anions) in a CH_3CN medium (Fig. 5d). Such variation in counter ions showed no detectable impact on the response of **1** towards Hg^{2+} ions. This is indeed an important observation, as in many cases, interference from counter anions can hinder the accuracy of the sensor molecules. Since Hg^{2+} contamination can be encountered in various types of industrial waste materials, we examined the responses of compound **1** towards Hg^{2+} ions in different organic solvents, such as CH_3CN, THF, and DMF (Fig. 5b). The degree of response, as denoted by changes in absorbance at the 427 nm band, were found to be maximum in THF, followed by CH_3CN and DMF. In less polar solvents such as THF, the interaction between Hg^{2+} ions and the probe will be stronger because Hg^{2+} ions are less solvated, making them more available to bind with the probe. However, DMF and CH_3CN could form Hg^{2+}-solvent complexes owing to the lone pairs on oxygen (DMF) or nitrogen (CH_3CN) atoms, which significantly reduce the interaction with Hg^{2+} ions.[15]

Since we studied interactions in a pure CH_3CN medium, we were interested to investigate the effect of water on Hg^{2+} sensing. It was observed that with increasing water content in the mixture, the response towards Hg^{2+} ions gradually decreased (Fig. 5c). The changes in absorbance (A/A_0) at the 427 nm band was found to be ~10-fold in 1 : 1 CH_3CN–H_2O mixture, while it was ~1.5-fold in pure water. This might be due to the extensive solvation of Hg^{2+} ions in water and aggregation of probe molecules through hydrogen bonding interaction.[16]

Mechanistic investigation with Hg^{2+} ions

The mode of binding with Hg^{2+} was unveiled using a series of spectroscopic investigations. The superior response of compound **1** towards Hg^{2+} compared to **2** ruled out the possible involvement of the hydrazo linker in the coordination with Hg^{2+} ions. Thus, it could be anticipated that Hg^{2+} in both cases is coordinated through the pyridyl nitrogen end. Irrespective of spectral response, both compounds showed 1 : 1 binding stoichiometry with Hg^{2+} ions in a CH_3CN medium (Fig. 6a). The Benesi–Hildebrand equation for the 1 : 1 model was utilized for calculation of binding constants (Fig. 6b). Compound **1** showed larger binding affinity ($\log K = 4.84 \pm 0.03$) towards Hg^{2+} ions than compound **2** ($\log K = 3.95 \pm 0.02$), which justified the larger optical response observed with the former probe. The reversible nature of Hg^{2+} coordination was verified using EDTA as the chelator agent.[17] First, Hg^{2+} (2 equiv.) was added to the solution of **1** (or **2**) and to that the same equivalent of EDTA was added, which completely revived the original spectrum of **1** (or **2**) (Fig. 6c). This suggested a reversible coordination between the probe molecules and Hg^{2+} ions. Moreover, this result indicated that a single solution of the probe (either **1** or **2**) can be used multiple times for the detection of Hg^{2+} ions. Since protonation of the pyridine moiety can facilitate charge transfer interaction, we compared the spectral response in the presence of both Hg^{2+} and H^+ (HCl) (Fig. 6d).[18] Both spectra resembled each other, which indicated that Hg^{2+} ions coordinated through the pyridine unit of the compound.

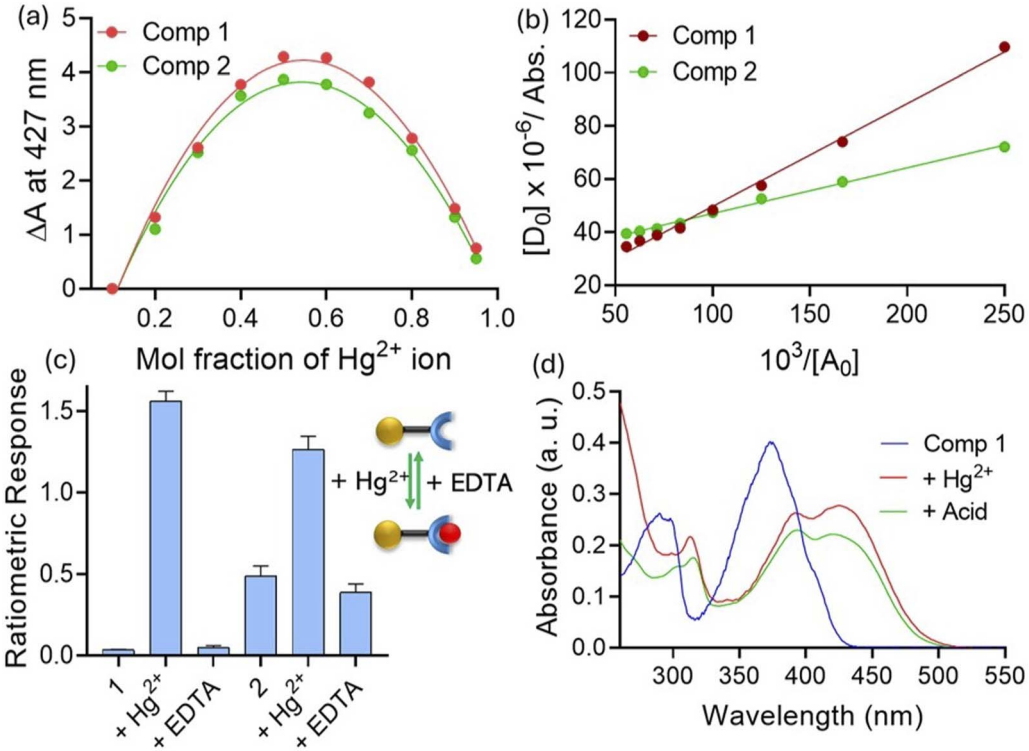

Fig. 6 (a) Job's plot of compounds **1** and **2** in the presence of Hg^{2+} ions. (b) Determination of binding constants of compounds **1** and **2** with Hg^{2+} ions. (c) Recovery experiment with EDTA showing the reversible interaction of **1** and **2**. (d) UV-visible spectra of **1** (10 μM) with different Hg^{2+} salts (25 μM) in a CH_3CN medium [each experiment was independently performed thrice for reproducibility].

Conclusion

This study highlights the design, synthesis, and evaluation of two prenylated probes for selective detection of Hg^{2+}, emphasizing the role of structural and electronic factors in determining sensing efficiency. The two probes, differing in their linker units, olefinic (compound **1**) and hydrazo (compound **2**), exhibited charge transfer interactions leading to visible color changes upon interaction with Hg^{2+} ions. Computational studies revealed planar structures and similar HOMO–LUMO energy gaps (~0.12 eV), while experimental UV-visible and fluorescence spectroscopy identified distinct optical responses. Compound **1** demonstrated superior sensitivity ($A/A_0 \sim 13$-fold) and a lower detection limit (1.2 ppm) compared to compound **2** ($A/A_0 \sim 2$-fold, 5.8 ppm), possibly owing to its less flexible linker and higher binding affinity for Hg^{2+} ions. Ratiometric responses ($r^2 > 0.99$) and excellent selectivity towards Hg^{2+} over other metal ions further established the efficacy of these probes for quantitative analysis. The environmental robustness of the probes was evaluated under varying conditions, including solvent polarity, water content, and counter-ion effects. Sensing efficiency decreased in high-water-content systems because of solvation effects and probe aggregation but remained consistent across different Hg^{2+} salts. Mechanistic investigations confirmed pyridine nitrogen as the primary coordination site, with 1 : 1 stoichiometry and reversible binding validated by EDTA recovery. Practical applicability was demonstrated using chemically modified paper strips, enabling cost-effective, user-friendly Hg^{2+} detection with quantitative image analysis. These findings underline the potential of structurally tuneable charge-transfer-based probes for developing reusable, sensitive, and selective optical sensors for heavy metal pollutants in diverse environments.

Data availability

Data are available from the author upon reasonable request.

Conflicts of interest

There are no conflicts to declare.

Acknowledgements

N. D. thanks DST for the SYST grant (SP/YO/2021/1632) and also thanks the Ministry of Education (MOE) for STARS grant (STARS-2/2023-0300).

References

1 A. Taha, N. Farooq, N. Singh and A. A. Hashmi, *J. Mol. Liq.*, 2024, **401**, 124678.
2 X. Wang, C. Shen, C. Zhou, Y. Bu and X. Yan, *Chem. Eng. J.*, 2021, **417**, 129125.

3 (*a*) S. Shakya and I. M. Khan, *J. Hazard. Mater.*, 2021, **403**, 123537; (*b*) R. S. Fernandes and N. Dey, *J. Mol. Liq.*, 2022, **367**, 120369.
4 (*a*) D. Shen, W.-C. Chen, M.-F. Lo and C.-S. Lee, *Mater. Today Energy*, 2021, **20**, 100644; (*b*) R. S. Fernandes and N. Dey, *Ind. Eng. Chem. Res.*, 2023, **62**, 21536–21545.
5 J. Jia, X. Wu, X. Zhang, Y. Wang, J. Yang, Y. Fang and Y. Song, *Phys. Chem. Chem. Phys.*, 2022, **24**, 955–965.
6 M. Baharfar, A. C. Hillier and G. Mao, *Adv. Mater.*, 2024, **36**, 2406083.
7 S. Sasaki, G. P. C. Drummen and G. Konishi, *J. Mater. Chem. C*, 2016, **4**, 2731–2743.
8 (*a*) Y. Singh, A. Gulyani and S. Bhattacharya, *FEBS Lett.*, 2003, **541**, 132–136; (*b*) N. Dey and S. Bhattacharya, *Dalton Trans.*, 2018, **47**, 2352–2359.
9 H. Oberhofer, K. Reuter and J. Blumberger, *Chem. Rev.*, 2017, **117**, 10319–10357.
10 S. Kumar, L. G. Franca, K. Stavrou, E. Crovini, D. B. Cordes, A. M. Z. Slawin, A. P. Monkman and E. Zysman-Colman, *J. Phys. Chem. Lett.*, 2021, **12**, 2820–2830.
11 (*a*) F. de Moliner, F. Nadal-Bufi and M. Vendrell, *Curr. Opin. Chem. Biol.*, 2024, **80**, 102458; (*b*) N. Dey, *Dalton Trans.*, 2021, **50**, 12563–12569.
12 X. Huang, J. Song, B. C. Yung, X. Huang, Y. Xiong and X. Chen, *Chem. Soc. Rev.*, 2018, **47**, 2873–2920.
13 A. Ko and C. Liao, *Anal. Methods*, 2023, **15**, 4377–4404.
14 (*a*) S. Patel, R. Jamunkar, D. Sinha, M. Patle, T. K. Patle, T. Kant, K. Dewangan and K. Shrivas, *Trends Environ. Anal. Chem.*, 2021, **31**, e00136; (*b*) B. Maiti, N. Dey and S. Bhattacharya, *ACS Appl. Bio Mater.*, 2019, **2**, 2365–2373.
15 (*a*) H. Li, J. Li, Z. Pan, T. Zheng, Y. Song, J. Zhang and Z. Xiao, *Spectrochim. Acta, Part A*, 2023, **291**, 122379; (*b*) H. V. Barkale and N. Dey, *Asian J. Org. Chem.*, 2024, **13**, e202300657.
16 M. Bogunia and M. Makowski, *J. Phys. Chem. B*, 2020, **124**, 10326–10336.
17 (*a*) P. Zhou, Q. Meng, G. He, H. Wu, C. Duan and X. Quan, *J. Environ. Monit.*, 2009, **11**, 648–653; (*b*) N. Dey, N. Kumari, D. Biswakarma, S. Jha and S. Bhattacharya, *Inorg. Chim. Acta*, 2019, **487**, 50–57.
18 S. Saha, A. De, A. Ghosh, A. Ghosh, K. Bera, K. S. Das, S. Akhtar, N. C. Maiti, A. K. Das, B. B. Das and R. Mondal, *RSC Adv.*, 2021, **11**, 10094–10109.